

## Electronic structure of Aurivillius phases: Ideal $\text{Bi}_2\text{NbO}_6$ , its stabilization with fluorine substitution and the role of oxygen vacancies

N. I. Medvedeva and S. A. Turzhevsky

*Institute of Solid State Chemistry, Ural Branch of Russian Academy of Sciences, Ekaterinburg, 620145, Russia*

V. A. Gubanov and A. J. Freeman

*Materials Research Center and Department of Physics and Astronomy, Northwestern University, Evanston, Illinois 60208*

(Received 1 July 1993)

The electronic structure of the first member of the Aurivillius family of phases  $\text{Bi}_2\text{O}_2(M_{m-1}\text{NbO}_{3m+1})$  with  $m=1$  has been calculated using the linear muffin-tin orbital (LMTO) method. The band structure of  $\text{Bi}_2\text{NbO}_6$  is similar to that of  $\text{Bi}_2\text{O}_3$ , which is the best oxygen ionic conductor. The Fermi level is located at the strong O  $2p$  peak and reveals the formation of a large number of oxygen holes in the valence band. The substitution of fluorine for oxygen is shown to lead to a stabilization of the structure and the formation of  $\text{Bi}_2\text{NbO}_5\text{F}$ . The preferred sites for fluorine substitution have been determined based on substitution energy estimates. The role of oxygen vacancies on the electronic structure and stability of the phases is investigated. Ideal  $\text{Bi}_2\text{NbO}_6$  is shown to be unstable and tends to contain a large number of oxygen vacancies. Vacancy formation energies have been found for different oxygen sites of the ideal crystals.

### I. INTRODUCTION

The layered perovskite transition-metal oxides are, at present, one of the most intensely studied groups of solids because of the continuing search for new high- $T_c$  superconducting materials with, hopefully, better characteristics than the known copper oxide systems. As this search develops more elaborate experimental techniques become available for the precise chemical synthesis of new phases and their physical and chemical investigations, unusual anomalies in the electrical, magnetic, and optical properties of such oxide phases are being found; these make them of great interest as electronic materials, ferroelectrics, sensors and ionic conductors, nonlinear optical materials, and other applications. One such group of oxides, to which considerable attention is being paid recently is the oxide Aurivillius phases discovered in the early 1950s.<sup>1</sup>

Interest in them has been revived in connection with the screening of copperless oxide systems with variable transition-metal valence, which, if similar to high- $T_c$  cuprates, might be considered as good candidates for superconducting materials. Among these systems, the most studied and intriguing are Bi- and Nb-based compounds. Recently, superconductivity in  $\text{Li}_x\text{NbO}_2$  (Ref. 2) and  $\text{NaNbO}_2$  (Ref. 3) have been discovered with  $T_c$ 's, of 5 and 4–5 K, respectively. Some indications of the possible occurrence of superconducting-phase inclusions in Sr-Nb-O with  $T_c$  up to 160 K (Refs. 4–5) systems cannot be completely excluded. An even more contradictory situation holds for Bi oxide systems: the cubic  $\text{Ba}_{1-x}\text{K}_x\text{BiO}_3$  copperless superconductor with  $T_c=30$  K was obtained quite a while ago. But except for these  $\text{BaPdO}_3$ – $\text{BaBiO}_3$ -based perovskites, no other Bi-containing copperless superconductor has been found since then, al-

though quite a number of new perovskite-like layered Bi-based compounds have been synthesized and investigated.<sup>6–10</sup> The reasons why the reduced dimensionality in the layered Bi-containing oxides does not favor superconductivity—in contrast to the cuprate case—are completely unclear at the moment; thus, theoretical investigations of possible electronic-structure peculiarities might give some insight.

Linearized augmented plane wave (LAPW) calculations<sup>11</sup> of the recently obtained layered compound  $\text{BaK}_{2-x}\text{Ba}_x\text{Bi}_2\text{O}_7$  (Ref. 10) suggest that for  $x=0.8$  some favorable conditions for high- $T_c$  superconductivity may exist in this material, which belongs to the Ruddlesden-Popper (RP) series  $A_{n+1}B_nO_{3n+1}$ , with  $n=2$ . It is worth noting that a number of known superconducting cuprates, namely  $(\text{La,Sr})_2\text{CuO}_4$ ,  $\text{Ba}_2\text{TlCuO}_5$ , and  $\text{Sr}_2\text{Bi}_2\text{CuO}_6$ , are representatives of these RP phases. As was shown in Refs. 12 and 13, the RP phases can be represented by a combination of  $v$  or  $v'$  perovskite ( $\text{La,Sr}$ , or  $\text{Ba}$ ) $\text{CuO}_3$  units and  $w$  or  $w'$   $MO$  ( $M=\text{La,Tl,Bi}$ ) units. In this way, the RP superconducting phase  $\text{Sr}_2\text{Bi}_2\text{CuO}_6$  can be represented by the simple schematic formula  $vw_3v'$ . The Aurivillius phases are very similar to the RP family and can be represented by combinations of  $V$  or  $V'$  perovskite (for example,  $\text{CaNbO}_3$ ) structural units and  $W'$  [for example,  $(\text{Bi,Nb})\text{O}_2$ ] structural units. Then, the Aurivillius phase  $\text{CaNb}_2\text{Bi}_2\text{O}_9$  can be easily presented as being of the  $VW_3V'$ -type.

Although the normal Aurivillius phases (AP) are usually semiconducting with the  $B$ -site metal in the undoped phase initially believed to be in the  $d^0$  state, valence fluctuations may be induced easily by chemical substitutions, and thus the variable transition-metal valences, which are believed to be one of the characteristic features of high- $T_c$  superconducting oxide compounds, can be realized.

In particular, new compounds like  $\text{LaBa}_2\text{Cu}_2\text{NbO}_8$  have been investigated recently,<sup>14</sup> and possible high- $T_c$  superconductivity has been suggested for doped  $\text{LaBa}_2\text{Cu}_2\text{Nb}(\text{Ta}, \text{Ti})\text{O}_8$  crystals. Moreover, the proposed superconductors may be obtained as the stacking of AP structural units and active  $\text{CuO}_2$  layers. Such similarities with the known RP family of compounds serve as the basis for suggestions<sup>15-17</sup> that there is a chance to find new superconductors, as well as compounds with unusual resistivity anomalies, among the Aurivillius phases, which are well known to exhibit ferroelectricity along with high-Curie temperatures.<sup>18</sup>

In this paper, we present results of theoretical modeling of the electron structure for the first, simplest representative of Nb-Bi Aurivillius phase,  $\text{Bi}_2\text{NbO}_6$ , and investigate the effects of the chemical substitution of oxygen, as well as oxygen vacancy formation, on the stability and peculiarities in the electronic structure of this compound.

## II. CRYSTALLOGRAPHIC MODELS AND CALCULATIONAL TECHNIQUES

The Aurivillius phases under consideration have tetragonal crystal lattices and consist of  $\text{Bi}_2\text{O}_2$  fluoritelike layers and perovskite layers, both of them arranged perpendicular to the  $c$  axis.<sup>19,20</sup> The  $M'$ -type metal in the phase having the general formula  $\text{Bi}_2\text{O}_2(M'_{m-1}R_m\text{O}_{3m+1})$  is twelve coordinated and is related to the  $A$  sites of the perovskite layers (usually Ca, Sr, Ba, Bi, Pb, Cd, La, Sm, Sc, etc.). Here  $R$  is the six-coordinated transition metal at the  $B$  perovskite site (Nb, Ti, Ta, W, Fe, etc.) and  $m$  in this formula is the number of layers. At present, the following phases are known in this Aurivillius family:  $\text{BaBi}_4\text{Ti}_4\text{O}_{15}$  (corresponding to  $m=4$ ),  $\text{Bi}_4\text{Ti}_3\text{O}_{12}$  ( $m=3$ ), and  $\text{CaBi}_2\text{Nb}_2\text{O}_9$  ( $m=2$ ). The tetragonal phase in this system with  $m=1$ , i.e.,  $\text{Bi}_2\text{Nb}_2\text{O}_6$ , appears to be unstable under the usual chemical synthetic approaches (likewise for the undoped body-centered-tetragonal bct phase  $\text{Ba}_2\text{BiO}_4$  in the tetragonal phase family  $\text{Ba}_{n+1}\text{Bi}_n\text{O}_{3n+1}$ , with  $n=1$ ) and has not been synthesized yet. However, the proper heat treatment of a  $\text{BiF}_3 + \text{Nb}_2\text{O}_5$  mixture<sup>20</sup> produced the well-characterized  $\text{Bi}_2\text{NbO}_5\text{F}$  compound, which implies that the stabilization of an undoped Aurivillius phase for  $m=1$  cannot be completely excluded under some special experimental conditions. For this reason we have studied in detail both the existing  $m=1$  fluorine-doped  $\text{Bi}_2\text{NbO}_5\text{F}$  and the model-undoped  $\text{Bi}_2\text{NbO}_6$  phases in order to estimate the role of fluorine in the stabilization of the  $m=1$  phase and to investigate the electronic-structure peculiarities of these, the simplest members of the Aurivillius phase family.

$\text{Bi}_2\text{NbO}_5\text{F}$  belongs to the  $I4/mmm$  space group with the lattice parameters  $a=3.835 \text{ \AA}$  and  $c=16.63 \text{ \AA}$ .<sup>20</sup> Atomic positions in the crystal lattice are given in Table I. Three nonequivalent oxygens are located in the niobium-oxygen plane O(1), apical position O(2), and in the  $\text{Bi}_2\text{O}_2$  layer O(3) (see Fig. 1). The oxygens surrounding the Nb atom form a distorted octahedron; Nb-O bonds for the in-plane oxygens (Fig. 1) are significantly shorter ( $1.92 \text{ \AA}$ ) than the bonds with apical oxygen atoms

TABLE I. Atom position parameters for  $\text{Bi}_2\text{NbO}_5\text{F}$

Atom	Type	$x$	$y$	$z$
Nb	$2a$	0	0	0
Bi	$4e$	0	0	0.325
(O,F)1	$4c$	0	0.5	0
(O,F)2	$4e$	0	0	0.12
(O,F)3	$4d$	0	0.5	0.25

( $2.0 \text{ \AA}$ ). The Bi-O(2) and Bi-O(3) distances are equal to  $2.29$  and  $2.9 \text{ \AA}$ , respectively. Since the position of oxygen and fluorine atoms cannot be distinguished either from the experimental x-ray-diffraction data or any qualitative spatial considerations, no assumptions were made in (Ref. 19) on the possible positions of the F atoms in the  $\text{Bi}_2\text{NbO}_5\text{F}$  crystal lattice. We have studied this problem making use of band-structure calculations.

The scalar relativistic version of the linear-muffin-tin orbital (LMTO) method<sup>21</sup> was employed with the von Barth-Hedin form<sup>22</sup> of exchange-correlation potential. The atomic sphere radii were chosen to be  $R_{\text{Bi}}=3.81 \text{ \AA}$ ,  $R_{\text{Nb}}=2.84 \text{ \AA}$ ,  $R_{\text{O}}=2.1 \text{ \AA}$ . In the substituted structures,  $R_{\text{F}}$  was taken to be  $2.1 \text{ \AA}$ . The oxygen-vacancy radius was taken to be equal to that of an oxygen. In all,  $18 k$  points were used in the integrations over the irreducible part of the Brillouin zone.

We have used band theory to investigate the relative stability and the preferable sites for fluorine substitutions and oxygen-vacancy formation. As is known, the cohesive energy of the crystal can be found as the difference between the total energy  $E_{\text{tot}}$  and the sum of the energies of free atoms forming the crystal. When full-potential methods (FLAPW or FLMTO) are used in local density functional theory, they usually give reliable estimates of the crystal cohesion. The LMTO technique with spherically symmetric potentials inside the atomic spheres must certainly result in lower accuracy. It appears, however, rather sufficient to provide good agreement of  $E_{\text{coh}}$  with experiment for large groups of transition-metal oxides, carbides, and nitrides.<sup>23,24</sup>

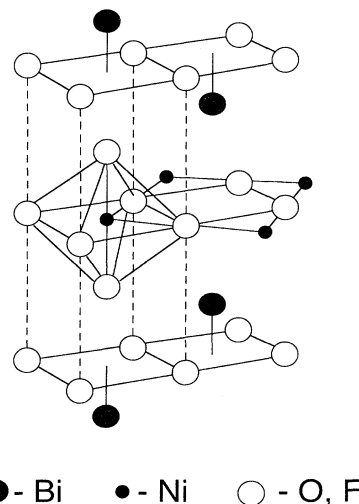


FIG. 1. Crystal structure of the  $m=1$   $\text{Bi}_2\text{Nb}(\text{O}, \text{F})_6$  Aurivillius phase.

Moreover, we use the relative changes of  $E_{\text{coh}}$  for compounds of the same structure and similar composition and the frozen-core approximation in order to get the relative changes of  $E_{\text{coh}}$  in a more correct way. As shown in Ref. 25, when calculating  $E_{\text{coh}}$ , some contributions to the valence energy of atoms from spin-spin, spin-orbit, and orbital-electron corrections should be taken into account. In our estimates of  $E_{\text{coh}}$ , we include only the largest spin-spin corrections as estimated by the difference of valence energies for spin-polarized and spin-restricted atomic states.

We have estimated the energy of formation of oxygen vacancies ( $E_{\text{vac}}$ ) and the substitution energy ( $E_{\text{sub}}$ ) of fluorine atoms for oxygen as the difference of  $E_{\text{coh}}$  values for both the defect compound and ideal  $\text{Bi}_2\text{NbO}_6$ . For the more correct estimate of these energies, it is necessary to take into account the corrections  $E_d$  for the dissociation of metalloid during the formation of a defect compound; while the corrections are rather small, they are comparable with the vacancy-formation and fluorine-substitution energies and should be taken into account. These estimates have been used to determine the preferred sites for oxygen-vacancy formation and for oxygen substitution for fluorine in the ideal  $\text{Bi}_2\text{NbO}_6$  Aurivillius phase.

### III. RESULTS AND DISCUSSION

#### A. Ideal $\text{Bi}_2\text{NbO}_6$

The total and partial densities of states for  $\text{Bi}_2\text{NbO}_6$  shown in Fig. 2 (not including the O 2s and Bi 6s subbands) give a general overview of the electronic properties of this compound. The wide band in the energy range from  $-0.8$  up to  $-0.2$  Ry is a strongly hybridized Bi(6p) Nb(4d), and O(2p) band. The hybridization of Bi 6p states with the O 2p states of the O(3) atoms in the  $\text{Bi}_2\text{O}_2$  fluorite layers determines the shape of the lower part of the valence band. The bonding of Bi atoms with O(2) as well as with oxygen atoms in the Nb-O planes is negligible. Strong hybridization of Nb 4d states with O(1), O(2), 2p orbitals defines the shape of the central part of the valence band, while the upper part is mainly of weakly bonding O(1), O(2) 2p states. The Fermi level falls onto the intense peak formed almost exclusively from oxygen 2p states: the main contributions to  $N(E_F)$  arise from O(1) 2p and, especially, apical O(2) 2p states; contributions of oxygen atoms from the Bi-O(3) planes are an order of magnitude smaller (cf. Table II); Nb 4d states do not appear at  $E_F$ .

Our conclusions about the nature of the lowest unoccupied states are very similar to the results of LAPW calculations<sup>26</sup> for the body-centered-tetragonal bct  $\text{Ba}_{n+1}\text{Pb}_n\text{O}_{3n+1}$  series of compounds; they appear to have apical oxygen character. The density-of-states DOS diagram in Fig. 2 gives an idea of the large amount of oxygen holes, especially at the apical O(2) sites, which can appear in the phase under consideration. In this respect, the band structure of  $\text{Bi}_2\text{NbO}_6$  is very much like that of  $\delta\text{-Bi}_2\text{O}_3$ , (Ref. 17), which is one of the best known oxygen ionic conductors and crystallizes in the defect fluorite structure. At the same time, it is obvious, just from Fig.

2 alone, that with  $E_F$  located at the narrow and very intense maximum of the DOS,  $\text{Bi}_2\text{NbO}_6$  has to be very unstable. Thus, a shift of  $E_F$  to the lower DOS region due to the distortions of the crystal lattice, vacancy formation, or substitutions would provide an essential stabilizing effect on this  $m = 1$  phase. It is worth noting that just above  $E_F$  there is an antibonding oxygen peak at  $-0.13$  Ry, similar to the one in the Bi-containing superconductor. The main contributions to this peak are due to the hybridized Bi 6p-O(3) 2p states in fluorite layers, along with small contributions from Nb 4d (1 state/Ry spin) and 2p apical oxygen states (2 states/Ry spin). It cannot be excluded that the shift of  $E_F$  to this peak (for example, through intercalation of the structure by alkali-metal atoms) might result in some favorable conditions for the appearance of superconducting properties of such a crystal.

#### B. $\text{Bi}_2\text{NbO}_5\text{F}$

In order to understand why the fluorinated  $\text{Bi}_2\text{NbO}_5\text{F}$  phase can be rather easily obtained—as opposed to

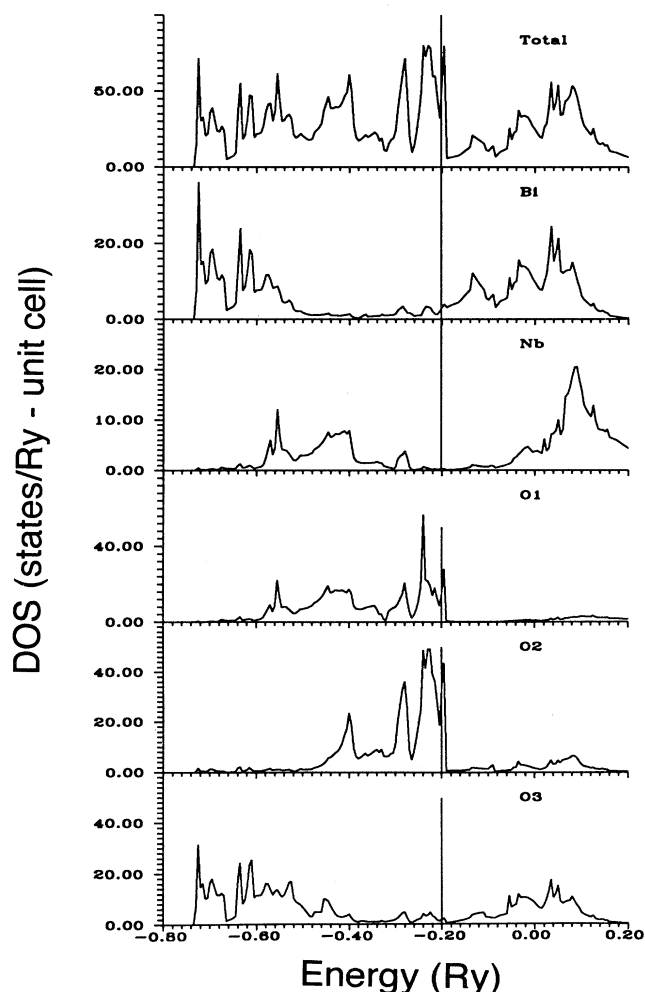


FIG. 2. Total and partial densities of states for ideal  $\text{Bi}_2\text{NbO}_6$ .

TABLE II. Total energy  $E_{\text{tot}}$ , cohesive energy  $E_{\text{coh}}$ , Fermi level  $E_F$ , and the total and partial densities of states at  $E_F$  (in states/Ry spin).

		$\text{Bi}_2\text{NbO}_6$	$\text{Bi}_2\text{NbO}_5\text{F}(1)$	$\text{Bi}_2\text{NbO}_5\text{F}(2)$	$\text{Bi}_2\text{NbO}_5\text{F}(3)$
$E_{\text{tot}}$ (Ry)		-229.263	-245.861	-245.970	-245.727
$E_{\text{coh}}$ (Ry)		-1.593	-1.483	-1.538	-1.416
$E_{\text{sub}}$ (Ry)		...	0.110	0.055	0.177
$E_F$ (Ry)		-0.200	-0.177	-0.191	-0.189
Total $N(E_F)$		54.79	20.99	33.73	65.66
Partial $N(E_F)$	Bi( $p$ )	3.21	1.81	5.19	7.05
	Nb( $d$ )	0.29	0.27	0.25	0.37
	O1( $p$ )	15.07	2.89	11.78	17.34
	O2( $p$ )	33.14	14.48	13.76	37.23
	O3( $p$ )	1.70	0.92	1.29	1.18
	F( $p$ )	...	0.05	0.22	0.79

$\text{Bi}_2\text{NbO}_6$ —we have carried out band-structure calculations for the fluorinated  $m=1$  Aurivillius phase, where fluorine atoms substitute different nonequivalent oxygen sites. The results are presented in Fig. 3 and Table II.

As is seen, fluorine substitution for different oxygens results in different changes of the electronic states: substitution of O(1) and O(2) atoms leads to the change of the states' distribution mainly near the Fermi level, but when fluorine replaces the O(3) atoms in the  $\text{Bi}_2\text{O}_2$  layers, the main changes appear in the lower part of the valence band only (Fig. 3). Thus, except for F(3)-type substitution, the appearance of fluorine at the oxygen site results in a drastic decrease of  $N(E_F)$ , which indicates structure stabilization. The calculated values of their total energies show the possibility of lattice stabilization with fluorine substitution, when fluorine atoms are located in O(2) positions, as is obviously seen from its  $E_{\text{coh}}$  value, which is the lowest. It follows from estimates of substitution energies  $E_{\text{sub}}$  that fluorine can substitute O(2) atoms with an energy that is two times less than that needed to substitute for O(1) atoms, or more than three times less than the energy for O(3) substitution.

The  $E_{\text{sub}}$  values obtained also explain the higher rela-

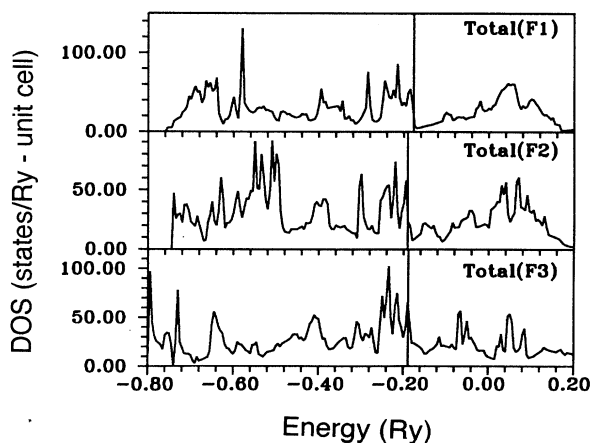


FIG. 3. Total densities of states for the fluorinated  $m=1$  Aurivillius phase  $\text{Bi}_2\text{NbO}_6\text{F}$  with fluorine atoms placed at the O(1), O(2), and O(3) sites (F1, F2, and F3, respectively).

tive stability of  $\text{Bi}_2\text{NbO}_5\text{F}$  found in (Ref. 20). Note that the  $E_{\text{sub}}$  values in Table II are given without  $E_d$  corrections. If these are taken into account [ $E_d = -0.05-0.10$  Ry (Ref. 23)], then  $E_{\text{sub}}$  for O(2) is negative, and fluorine substitution for O(2) atoms becomes energetically favorable and results in the formation of the fluorinated  $m=1$  phase. Most probably this type of process has been realized in (Ref. 20), when the  $\text{BiF}_3$  and  $\text{Nb}_2\text{O}_5$  mixture was heated to  $640-800^\circ\text{C}$  and then annealed for 7–15 h.

In Fig. 4 we present the partial densities of states calculated for this fluorinated phase; in Table II, the structure of the states at  $E_F$  is given. The drastic decrease of

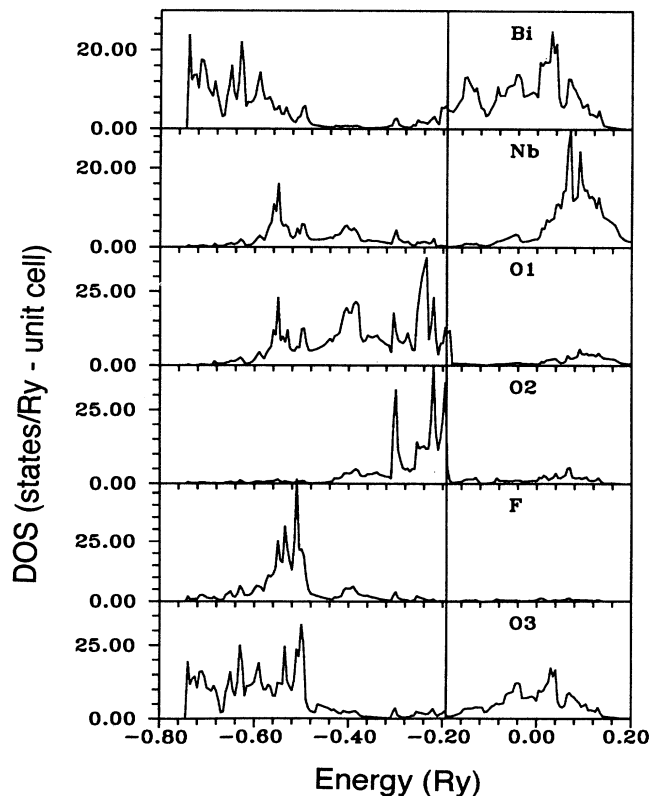


FIG. 4. Partial densities of states for  $\text{Bi}_2\text{NbO}_5\text{F}$  with the most energetically favorable position F2, of fluorine atoms.

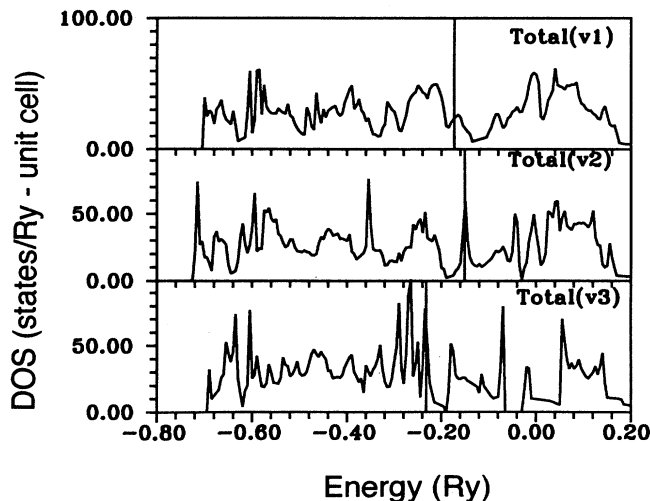


FIG. 5. Total densities of states for  $\text{Bi}_2\text{NbO}_5(\text{Vac})$  phase with oxygen vacancies located at O(1), O(2), and O(3) positions ( $v1$ ,  $v2$ ,  $v3$ , respectively).

the density of apical O(2)  $2p$  states at  $E_F$  as compared with  $\text{Bi}_2\text{NbO}_6$  is seen; the Fermi level is located at the upper slope of the O(1)  $2p$  and O(2)  $2p$  peaks and the number of oxygen holes in the fluorinated phase appears to be much decreased. A consequence might be not only the decreased conductivity of the fluorinated  $m=1$  Aurivillius phase, but a deterioration of oxygen ionic conductivity, which is likely to be high for  $\text{Bi}_2\text{NbO}_6$ .

### C. Oxygen vacancies in $\text{Bi}_2\text{NbO}_6$

The other common way to stabilize oxide phases is through the occurrence of oxygen vacancies. We have studied this possibility for  $\text{Bi}_2\text{NbO}_6$  making use of the LMTO method, by placing empty spheres at O(1), O(2), and O(3) crystal sites. The total densities of states obtained for all three cases are given in Fig. 5, and the densities of states at  $E_F$  and energies of vacancy formation are given in Table III.

The appearance of vacancies at different oxygen sites results in a rather different redistribution of states near  $E_F$ . The creation of oxygen vacancies in the Nb-O plane

$V(1)$ , leads to the formation of direct Nb-Nb bonds and the shift of Nb states to lower energy, so that the Nb  $4d$  contribution to  $N(E_F)$  increases by an order of magnitude (Table III). The total  $N(E_F)$  value drops by more than a factor of 2, which is in line with possible structure stabilization. As seen from the partial DOS at  $E_F$  (Table III), the compound becomes much more metallic; the contributions of oxygen states to  $N(E_F)$  are very much decreased in favor of metallic Nb  $4d$  states.

The energy bands calculated for  $\text{Bi}_2\text{Nb}_5V(1)$  plotted along the high-symmetry directions of the bct Brillouin zone are presented in Fig. 6. The band dispersion along  $\Gamma-Z$  ( $c$  axis) is minimal and the bands are of nearly two-dimensional character. The Fermi level crosses the antibonding  $\sigma^*$  band with its energy minimum at  $X$ . This band is partially filled and consists of Nb  $4d$  (0.32–0.43) and vacancy  $2s$  (0.29–0.35) states. Since octahedrally coordinated Nb ( $5+$ ) ions are usually strongly bonded both with plane and apical oxygens, the creation of vacancies in these positions should be energetically unfavorable. Indeed, our calculated vacancy formation energies  $E_{\text{vac}}$  (cf. Table III) confirm this qualitative anticipation.

The creation of oxygen vacancies at O(2) brings the hybridized Bi-O(3) states to  $E_F$ , so that the contributions of the atoms from the fluorite layer—Bi  $p$  and O(3)  $2p$  states—define the  $N(E_F)$  composition for this type of structure. The smallest changes in  $N(E_F)$ , as compared with ideal  $\text{Bi}_2\text{NbO}_6$ , occur with the formation of oxygen vacancies at the O(3) position in the Bi-O fluorite layer. As is seen from the vacancy-formation energies presented in Table III, the O(3)-type of vacancy is preferred; the formation energy has a minimum value for this particular case. Moreover, if we taken into account the  $E_d$  correction,  $E_{\text{vac}}$  for O(3) becomes close to zero. This indicates that the formation of oxygen vacancies in the fluoritelike  $\text{Bi}_2\text{O}_2$  layer in the  $\text{Bi}_2\text{NbO}_6$  Aurivillius phase is energetically favorable and that such a phase should contain some definite amount of O(3) vacancies.

This is not too surprising. As is known, the best oxygen ionic conductors have cubic fluorite structures, which usually contain a large amount of oxygen vacancies, and with the growth of their number, the oxygen conductivity usually increases. For example, the ionic conductivity of  $\text{ZrO}_2$  is greatly enhanced when doped with low-valent metal oxides, which is believed to be due

TABLE III. Total energy  $E_{\text{tot}}$ , cohesive energy  $E_{\text{coh}}$ , Fermi level  $E_F$ , energy of vacancy formation  $E_{\text{vac}}$ , and the total and partial densities of states at  $E_F$  (in states/Ry spin).

	$\text{Bi}_2\text{NbO}_5V(1)$	$\text{Bi}_2\text{NbO}_5V(2)$	$\text{Bi}_2\text{NbO}_5V(3)$
$E_{\text{tot}}$ (Ry)	-196.606	-196.734	-197.095
$E_{\text{coh}}$ (Ry)	-1.290	-1.355	-1.535
$E_{\text{vac}}$ (Ry)	0.30	0.24	0.058
$E_F$ (Ry)	-0.173	-0.151	-0.229
Total $N(E_F)$	23.31	53.35	49.44
Partial $N(E_F)$			
Bi( $p$ )	1.13	23.15	10.78
Nb( $d$ )	4.27	1.77	0.46
O1( $p$ )	2.33	3.12	10.75
O2( $p$ )	9.1	6.84	21.89
O3( $p$ )	0.81	8.29	1.85

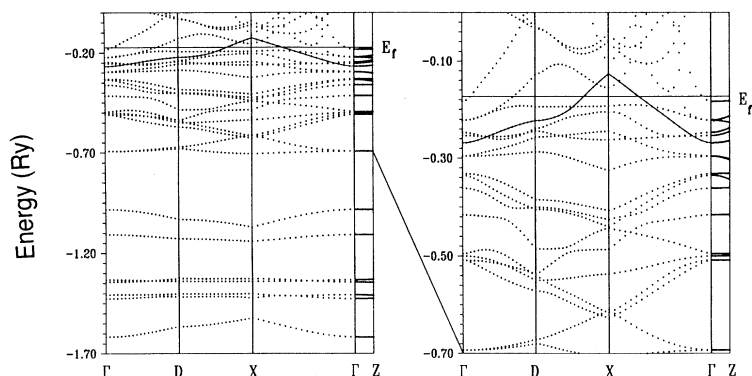


FIG. 6. LMTO energy bands for  $\text{Bi}_2\text{NbO}_5v_1$  along the symmetry directions of the bct Brillouin zone.

to the creation of additional oxygen vacancies. But this is not the case with  $\text{Bi}_2\text{O}_3$ , which already includes a large amount of oxygen vacancies (two oxygen vacancies per unit cell), and any attempt to stabilize its fluorite phase at room temperature by adding aliovalent oxides results in lowering the conductivity. The LMTO calculations for  $\delta\text{-Bi}_2\text{O}_3$  (Ref. 27), similar to the ones carried out for  $\text{Bi}_2\text{NbO}_6$  in this paper, showed that the existence of vacancies in  $\delta\text{-Bi}_2\text{O}_3$  is energetically favorable; Bi-O bands there are rather weak, can easily be broken, and the structure is stabilized mainly due to the formation of direct Bi-Bi bonds. As is seen from the above discussion, a very similar situation takes place in the  $m=1$  Aurivillius phase. All of this shows that if stabilized, the  $\text{Bi}_2\text{NbO}_6$  phase will certainly contain a large amount of oxygen vacancies in the  $\text{Bi}_2\text{O}_2$  layers and will be a good oxygen ionic conductor. The easy reduction of the  $\text{Bi}_2\text{O}_2$  layer was recently proved in the temperature investigations of the  $m=3$  titanium Aurivillius phase  $\text{Bi}_4\text{Ti}_3\text{O}_{12}$  (Ref. 18), when Bi metal was always easily detected.

It is worth noting that the  $\text{Bi}_2\text{NbO}_6$  phase studied here is isostructural with a number of lanthanide tungstates,  $L_2\text{WO}_6$  ( $L=\text{Pr, Nd, Sm, Eu, Gd, Tb, Dy}$ ) (Ref. 28), which are  $m=1$  Aurivillius phases. Hence, the possibility exists to obtain also some Bi-free Nb phases with more stable  $L_2\text{O}_2$  fluorite layers.

#### IV. CONCLUSIONS

The LMTO band-structure calculations have shown that due to certain electronic-structure peculiarities (high-density of states at  $E_F$ , low-cohesion energy)  $\text{Bi}_2\text{NbO}_6$ , the  $m=1$  phase of the Aurivillius family, is unstable and hence, difficult to obtain as an ideal phase. Oxygen substitution by fluorine leads to the stabilization of the  $\text{Bi}_2\text{NbO}_5\text{F}$  Aurivillius phase, with F atoms taking the place of apical oxygens in the Nb- $\text{O}_6$  distorted octahedra. The stabilization can also be achieved by the formation of oxygen vacancies, which are preferably created in fluorite  $\text{Bi}_2\text{O}_2$  layers and result in the enhanced ionic conductivity of this phase. Superconductivity is not expected in the fluorinated or defected  $\text{Bi}_2\text{NbO}_6$  structures, although the intercalation of  $\text{Bi}_2\text{NbO}_6$  with alkaline atoms, if feasible, might create some favorable conditions for the appearance of superconducting properties.

#### ACKNOWLEDGMENTS

Work at Northwestern University was supported by the National Science Foundation (through the Materials Research Center, Grant No. DMR 91-20521, and a computing grant at the Pittsburgh Supercomputing Center supported by its Division of Advance Scientific Computing).

<sup>1</sup>B. Aurivillius, *Ark. Kemi* **1**, 463 (1950); **1**, 499 (1950).

<sup>2</sup>M. J. Geselbracht, T. J. Richardson, and A. M. Stacy, *Nature* (London) **345**, 324 (1990).

<sup>3</sup>D. G. Kellerman *et al.*, *Superconductivity* **5**, 961 (1992).

<sup>4</sup>S. Matsuda *et al.*, *Jpn. J. Appl. Phys.* **29**, L1781 (1990).

<sup>5</sup>A. V. Mitin, G. M. Kuzmicheva, and E. P. Hlibov, *Superconductivity* **4**, 81 (1991).

<sup>6</sup>R. J. Cava, H. Takagi, H. W. Zandbergen, B. Hessen, J. J. Kraewski, and W. F. Peck, *Phys. Rev. B* **46**, 14 101 (1992).

<sup>7</sup>W. T. Fu *et al.*, *Soild State Commun.* **70**, 1117 (1989).

<sup>8</sup>K. Kourtakis and M. Robbins, *Mater. Res. Bull.* **24**, 1287 (1989).

<sup>9</sup>Q. Xu, T. Fu, J. M. van Ruitenbeek, and L. J. de Longh, *Physica C* **167**, 279 (1990).

<sup>10</sup>R. J. Cava, T. Siegrist, W. F. Peck, Jr., J. J. Krajewski, B. Batlogg, and J. Rosamilia, *Phys. Rev. B* **44**, 9746 (1991).

<sup>11</sup>L. F. Mattheiss, *Phys. Rev. B* **45**, 12 528 (1992).

<sup>12</sup>S. N. Ruddlesden and P. Popper, *Acta Crystallogr.* **10**, 538 (1957).

<sup>13</sup>S. N. Ruddlesden and P. Popper, *Acta Crystallogr.* **11**, 54 (1958).

<sup>14</sup>L. E. Mattheiss, *Phys. Rev. B* **45**, 2442 (1992).

<sup>15</sup>J. Hauck, K. Mika, and G. Krabbes, *Physica C*, **185-189**, 721 (1991).

<sup>16</sup>W. Zhou, P. A. Andersen, C. Lin, and P. Edwards, *Physica C*, **190**, 59 (1991).

<sup>17</sup>N. E. Alekseevskij and A. V. Mitin, *Superconductivity* **5**, 178 (1992).

<sup>18</sup>R. W. Wolfe, R. E. Newnham, and M. I. Kay, *Ferroelectrics* **3**, 62 (1971).

<sup>19</sup>B. Aurivillius and *Ark. Kemi*, **2**, 519 (1951).

<sup>20</sup>B. Aurivillius and *Ark. Kemi*, **5**, 39 (1952).

- <sup>21</sup>O. Gunnarsson, O. Jepsen, and O. K. Andersen, *Phys. Rev. B* **12**, 7144 (1983).
- <sup>22</sup>O. Gunnarsson and B. I. Lundquist, *Phys. Rev. B* **13**, 4274 (1976).
- <sup>23</sup>V. P. Zhukov, N. I. Medvedeva, and V. A. Gubanov, *Phys. Status Solidi B* **151**, 407 (1989).
- <sup>24</sup>N. I. Medvedeva, V. P. Zhukov, V. A. Gubanov, and M. Ya. Khodos, *Phys. Status Solidi B* **160**, 517 (1990).
- <sup>25</sup>M. S. Brooks *J. Phys. F* **7**, 613 (1977).
- <sup>26</sup>L. F. Mattheiss, *Phys. Rev. B* **42**, 359 (1990).
- <sup>27</sup>V. A. Gubanov and N. I. Medvedeva, *Physica B* **172**, 285 (1991).
- <sup>28</sup>G. Blasse, *J. Inorg. Nucl. Chem.* **28**, 1488 (1966).